

## Pyrolysis of Methyl *tert*-Butyl Ether (MTBE). 2. Theoretical Study of Decomposition Pathways

Taichang Zhang,<sup>†</sup> Lidong Zhang,<sup>†</sup> Jing Wang, Tao Yuan, Xin Hong, and Fei Qi\*

National Synchrotron Radiation Laboratory, University of Science and Technology of China, Hefei, Anhui 230029, P. R. China

Received: April 25, 2008; Revised Manuscript Received: June 30, 2008

The thermal decomposition pathways of MTBE have been investigated using the G3B3 method. On the basis of the experimental observation and theoretical calculation, the pyrolysis channels are provided, especially for primary pyrolysis reactions. The primary decomposition pathways include formation of methanol and isobutene, CH<sub>4</sub> elimination, H<sub>2</sub> elimination and C–H, C–C, C–O bond cleavage reactions. Among them, the formation channel of methanol and isobutene is the lowest energy pathway, which is in accordance with experimental observation. Furthermore, the secondary pyrolysis pathways have been calculated as well, including decomposition of *tert*-butyl radical, isobutene, methanol and acetone. The radicals play an important role in the formation of pyrolysis products, for example, *tert*-butyl radical and allyl radical are major precursors for the formation of allene and propyne. Although some isomers (isobutene and 1-butene, allene and propyne, acetone and propanal) are identified in our experiment, these isomerization reaction pathways occur merely at the high temperature due to their high activation energies. The theoretical calculation can explain the experimental results reported in part 1 and shed further light on the thermal decomposition pathways.

### 1. Introduction

MTBE is used as the most common gasoline additive, due to its excellent antiknock characteristic and cost-effective. The thermal decomposition of MTBE has been of considerably practical and theoretical interest. Moreover, the investigation of the relationship between MTBE molecular structure and its characteristics is helpful to find out more perfect additives. Its pyrolysis,<sup>1,2</sup> oxidation,<sup>3–8</sup> and combustion<sup>9,10</sup> have been extensively studied. Choo and co-workers suggested a four-center transition state for the decomposition of MTBE using the very low-pressure pyrolysis (VLPP) technique at 890–1160 K.<sup>1</sup> Dunphy and co-workers studied the high temperature oxidation of MTBE and binary mixture of methanol + isobutene at the temperature range of 1040–1850 K using the shock tube method and found that the two kinds of reactants presented similar characteristics in fuel-rich conditions.<sup>6</sup> Hence, they concluded that the decomposition of MTBE to methanol + isobutene is the main reaction pathway. Brocard et al. studied the reaction of MTBE with oxygen around 723 K and found formaldehyde and *t*-C<sub>4</sub>H<sub>9</sub> radical as a main reaction,<sup>3</sup> which does not present an oxidation reaction and appears as a thermal degradation.<sup>3</sup> Although different reaction channels were presented on the basis of the experimental measurements, theoretical studies on MTBE decomposition are few. Only the hydrogen abstraction from MTBE by hydroxyl radical was theoretically studied using the ab initio method.<sup>11</sup>

A comprehensive pyrolysis study of MTBE has been performed with molecular-beam mass spectrometry and tunable synchrotron VUV photoionization techniques.<sup>12</sup> A lot of new intermediates have been detected. Furthermore, isomers are identified by the measurements of photoionization efficiency spectrum. This work, as part 2, is to elucidate the decomposition

channels of MTBE with the high level ab initio calculation method G3B3. The decomposition pathways of MTBE and consequent reactions are discussed in detail.

### 2. Computational Method

The high precise calculation method G3B3<sup>13,14</sup> was employed to study the decomposition pathways of MTBE. It is an approximation for the QCISD(T,E4T)/G3large energy. It involves single-point calculations at the QCISD(T,E4T)/6-31G(d), MP4/6-31+G(d), MP4/6-31G(2df,p) and MP2(Full)/G3large levels, all carried out with the structures optimized at the B3LYP/6-31G(d) level. The ZPE from the frequency calculation is at the same level, scaled by 0.96. A small semiempirical correction is also applied to account for the high level correlation effect. All the calculations were performed with the Gaussian 03 program.<sup>15</sup> Relative energies and optimized geometries of the compounds and pertinent transition states are shown in Figures 1–9.

### 3. Results and Discussion

**3.1. Primary Pyrolysis Pathways.** Relative energies of the primary pyrolysis species and the transition states involved in the pyrolysis of MTBE are presented in Figures 1 and 2, which characterize the reaction profiles and elucidate the decomposition pathways. The optimized geometries of the reactant, transition states, intermediates and products are displayed in Figures 3–5.

**3.1.1. Isobutene + Methanol.** The lowest energy pathway is the decomposition of MTBE to methanol and isobutene (PC1) via a four-member-ring transition state TS1, which is in accord with previous works.<sup>1</sup> The energy barrier for this channel is only 62.70 kcal/mol. In our experimental study, the initial formation temperature ( $T_F$ ) of methanol and isobutene is 730 K, which is the lowest one among all the pyrolysis products.<sup>12</sup> This reaction includes the C2–O and C3–H bond cleavages and the O–H(C3) bond formation. The C2–O, O–H(C3) and

\* Corresponding author. E-mail: fqi@ustc.edu.cn. Fax: +86-551-5141078. Tel: +86-551-3602125.

<sup>†</sup> Both have the same contribution to this work.

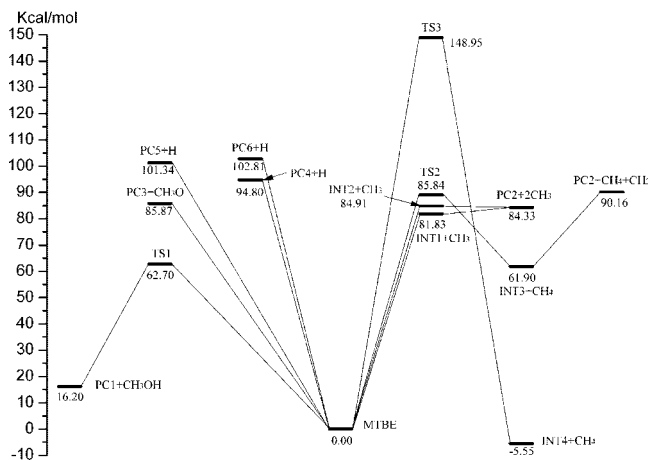


**Figure 1.** Relative energy of the primary species involved in the pyrolysis of MTBE calculated at the G3B3 level.

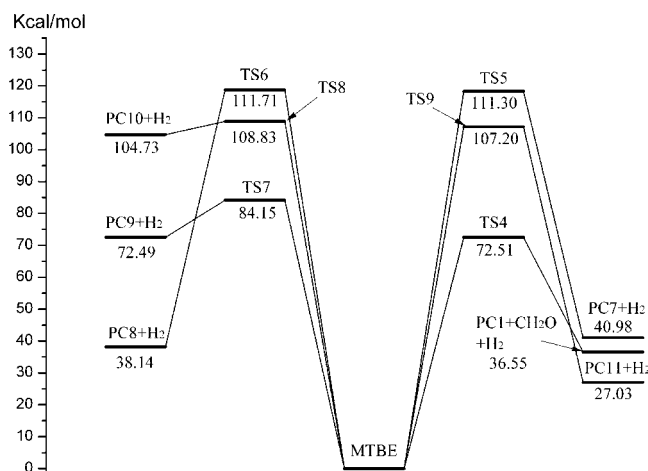


**Figure 2.** Relative energy of the primary species involved in H<sub>2</sub> elimination of MTBE calculated at the G3B3 level.

C3–H bond lengths in **TS1** are 2.107, 1.337 and 1.322 Å, respectively. The C2–C3 bond changes from single bond to double bond along with the bond cleavage and formation, and the C2–C3 bond lengths in MTBE, **TS1** and **PC1** are 1.533, 1.422 and 1.337 Å, respectively.

**3.1.2. Methoxy + *tert*-butyl Radicals.** MTBE can also dissociate directly to produce *tert*-butyl radical (**PC3**) and methoxy radical. The calculated dissociation energy (85.87 kcal/mol) is 23.17 kcal/mol higher than the barrier (**TS1**) for the lowest energy pathway (**PC1** + CH<sub>3</sub>OH). The methoxy radical can be detected at 890 K, and this channel will become effective above this temperature by competing with the four-center methanol elimination pathway. Although the *tert*-butyl radical is not detectable in our experiment,<sup>12</sup> the theoretical calculation reveals that the *tert*-butyl radical is ready to dissociate to isobutene on the basis of a relatively low dissociation energy (34.51 kcal/mol) of the dehydrogenation of the *tert*-butyl radical to produce isobutene, as shown in Figure 6. Meanwhile, Figure 6 presents other consumption channels of the *tert*-butyl radical, which is discussed in detail in the Secondary Pyrolysis section.

**3.1.3. Acetone Formation.** As shown in Figure 1, there are three pathways to form acetone from MTBE pyrolysis. (1) The *tert*-butoxyl radical (**INT1**) is produced by C1–O homolysis with 81.83 kcal/mol dissociation energy, and then acetone is formed via methyl loss from the *tert*-butoxyl radical. (2) The energy for C–C bond cleavage to form CH<sub>3</sub> and (CH<sub>3</sub>)<sub>2</sub>COCH<sub>3</sub> (**INT2**) radicals is 84.91 kcal/mol, which is 3.08 kcal/mol higher

than that of **INT1** formation. Subsequently, **INT2** forms stable acetone by further CH<sub>3</sub> elimination. (3) The H atom on C1 in MTBE can migrate toward one C atom of the CH<sub>3</sub> groups to produce **INT3** via a five-center transition state **TS2** with a barrier of 107.20 kcal/mol. The C4/C5–C2, C4/C5–H and C1–H bond lengths are 2.486, 1.372 and 1.419 Å in **TS2**, respectively. The C1–O and C2–O bond lengths (1.367 and 1.306 Å) in **INT3** are shorter than those in MTBE. The C–C bond cleavage occurs with the concomitant hydrogen transfer. Then acetone is formed via further dissociation of **INT3**.

**3.1.4. Methane + 2-Butanone.** The H atom of the *tert*-butyl group in MTBE migrates toward C1, yielding 2-butanone (**INT4**) via a five-center transition state **TS3** with a barrier of 148.95 kcal/mol. Although the energy of **INT4** + CH<sub>4</sub> is lower (–5.55 kcal/mol), the energy barrier for this channel is higher. Just at higher temperature this reaction channel can occur. On the other hand, 2-butanone can readily dissociate to other small species. Hence, the theoretical calculation suggests that 2-butanone should be very possible to be formed from pyrolysis of MTBE, which is in good agreement with our experimental study.<sup>12</sup>

**3.1.5. H Elimination Pathways.** Direct cleavage of C–H bonds of MTBE can occur at three different positions. These different C–H bond (C1–H, C3–H and C4/C5–H) cleavage energies are 94.80, 101.34 and 102.81 kcal/mol, corresponding to three different products, **PC4**, **PC5** and **PC6**, respectively. The C1–H bond cleavage energy is the lowest. Thus the first cleavage of C–H bond occurs at the C1–H bond, which shortens the C1–O bond from 1.413 to 1.360 Å. Compared with the C–O and C–C bond mentioned above, the C–H bond cleavage energies are higher. Thus the C–H bond cleavage does not have significant influence on MTBE pyrolysis.

**3.1.6. H<sub>2</sub> Elimination Pathways.** H<sub>2</sub> is detected as the major product in our MTBE pyrolysis experiment.<sup>12</sup> Figure 2 shows six different H<sub>2</sub> elimination pathways from MTBE. (1) The lowest barrier channel is dissociation of MTBE to **PC1**, formaldehyde and H<sub>2</sub> via a six-member-ring **TS4** over a barrier of 72.51 kcal/mol. The imaginary frequency is 1096.61 cm<sup>–1</sup> and the vibration model corresponds to the H<sub>2</sub> elimination. This reaction includes the C1–H, C2–O and C4/C5–H bond cleavage and H(C1)–H(C4/C5) bond formation. The C1–H, C2–O, C4/C5–H and H(C1)–H(C4/C5) bond lengths in **TS4** are 1.508, 2.289, 1.451 and 0.907 Å, respectively. (2) One H atom of the C3 in MTBE migrates toward one H atom of C4/C5, yielding **PC7** + H<sub>2</sub> via a five-center transition state **TS5** with a barrier of 111.30 kcal/mol. (3) Similar to channel 2, one H atom of the C4 in MTBE migrates toward one H atom of C5, yielding **PC8** + H<sub>2</sub> via a five-center transition state **TS6** with a barrier of 111.71 kcal/mol. (4) One H atom of C1 in MTBE migrates toward another H atom of C1, producing **PC9** + H<sub>2</sub> via a three-center transition state **TS7** over a barrier of 84.15 kcal/mol. (5) Direct H<sub>2</sub>-elimination of C3 in MTBE can occur via a three-member-ring transition state **TS8**, yielding triplet **PC10**. The barrier of this reaction is 108.83 kcal/mol. (6) H<sub>2</sub>-elimination of C4/C5 in MTBE can also occur via a three-member-ring transition state **TS9** with a barrier of 107.20 kcal/mol, yielding **PC11**. The barrier of channel 1 is much lower than those of the other channels mentioned above. Thus from the view of thermodynamics, channel 1 should play a significant role in H<sub>2</sub> formation. On the other hand, the other stable products including **PC7**, **PC8** and **PC11** could not be detected in our MTBE pyrolysis experiment, which indicates that channels 2, 3 and 6 have minor contributions in H<sub>2</sub> formation. For **PC9**

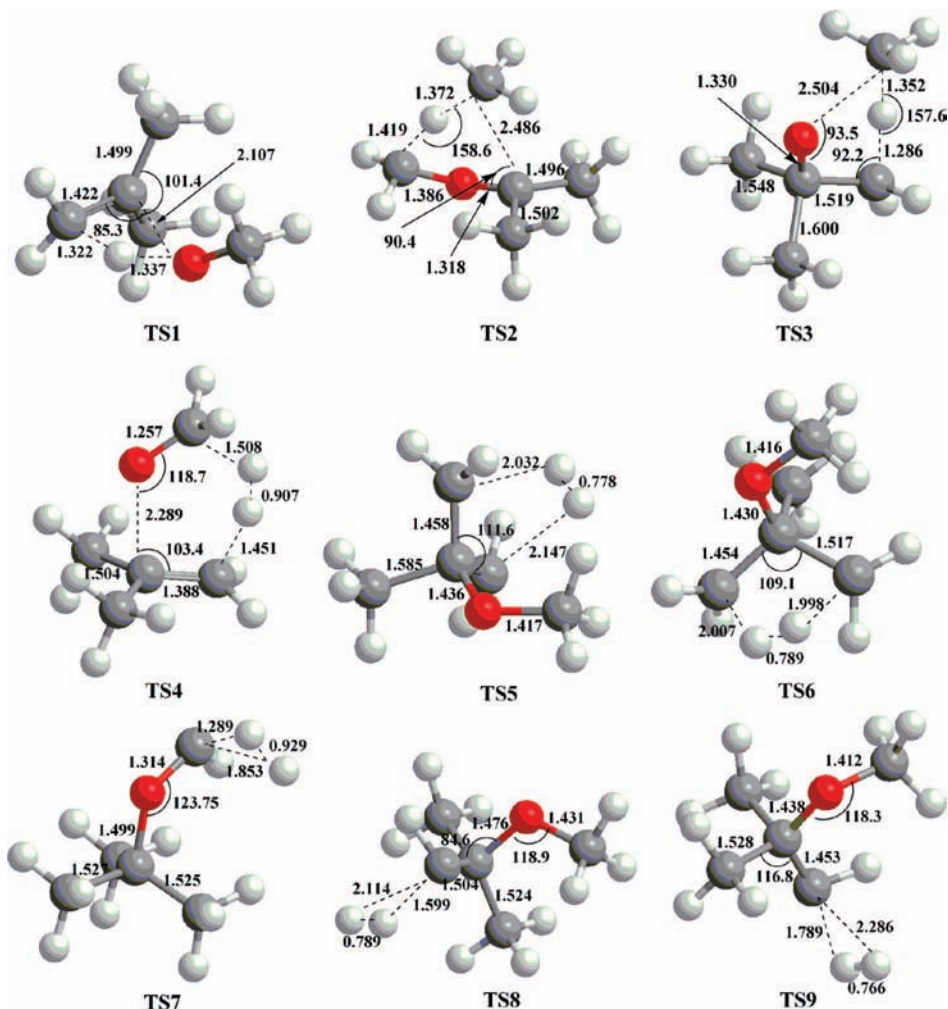


Figure 3. Optimized geometries of the transition states computed at the B3LYP/6-31G(d) level.

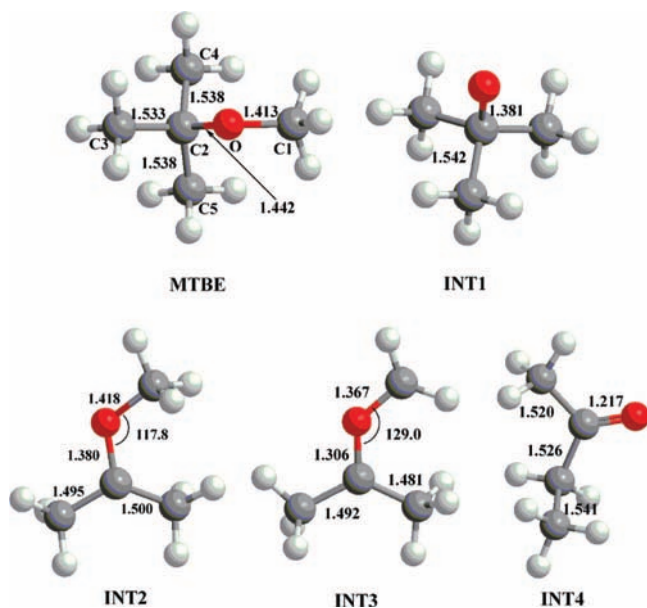


Figure 4. Optimized geometries of the reactant and intermediates computed at the B3LYP/6-31G(d) level.

and **PC10**, their unstable molecular structures can be readily destructed, making it hard to decide the importance of channels 4 and 5.

Besides the above-mentioned channels, direct dissociation of MTBE to isobutane was also calculated. The calculation results

show that this reaction is difficult. Thus isobutane identified in our experimental work should come from the combination of H with the *tert*-butyl radical.

**3.2. Secondary Pyrolysis Pathways.** The subsequent pyrolysis reactions of primary products can readily occur. Thus the study of the subsequent pyrolysis channels is desired. The *tert*-butyl radical, isobutene, methanol and acetone are the main products of primary decomposition of MTBE. Although pyrolysis of the *tert*-butyl radical,<sup>16–18</sup> isobutene,<sup>19</sup> methanol<sup>20,21</sup> and acetone<sup>22</sup> were previously studied by different groups, their works were mainly focused on the apparent active energy and rate constant of the lowest energy pathway. The information for other reaction pathways is lacking. Lin and co-workers calculated some major pathways for the unimolecular decomposition of methanol using G2 M theory,<sup>20</sup> and Zheng et al. calculated the lowest energy pathway of the *tert*-butyl radical decomposition using G3 and CBS methods.<sup>17</sup> Employing the G3B3 method the pyrolysis pathways of these secondary pyrolysis products are calculated and discussed in this work.

**3.2.1. Decomposition of the *tert*-Butyl Radical.** Figure 6 displays the decomposition pathways of the *tert*-butyl radical to isobutene, 1-butene, allene and propyne. The dissociation energy is 34.51 kcal/mol for the isobutene formation by H-elimination from the *tert*-butyl radical, which is consistent with that (33.83 kcal/mol) from Zheng and co-workers using the CBS method.<sup>17</sup> The *tert*-butyl radical can go through a three-center-ring transition state **TS10**, surmounting an energy barrier

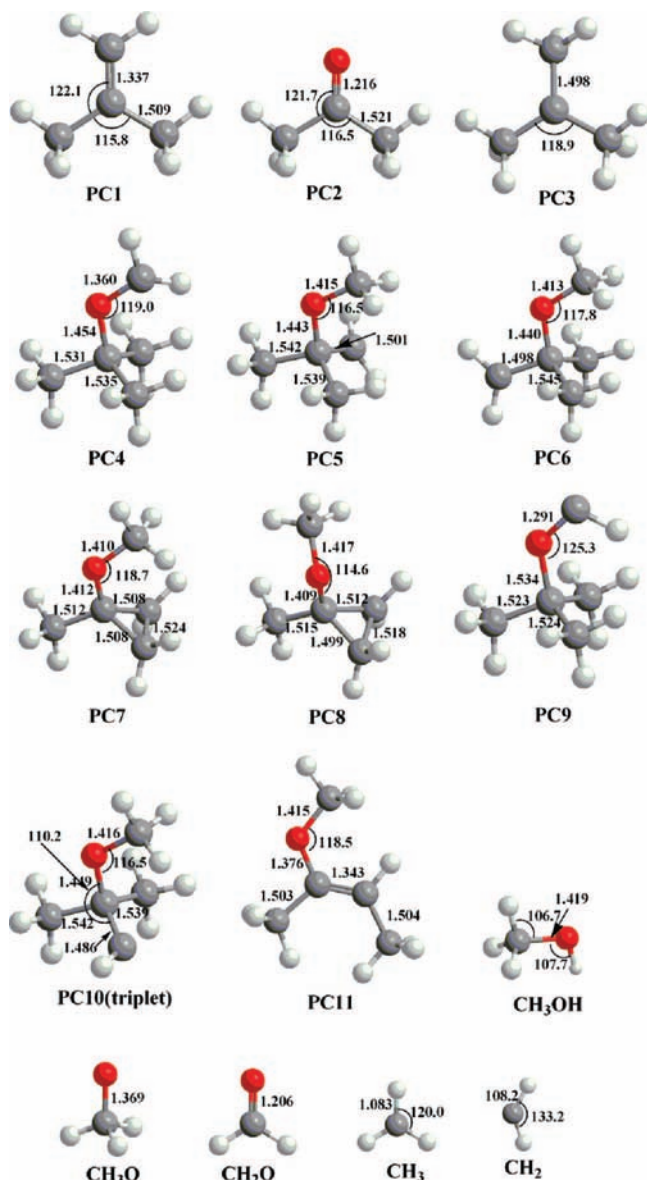


**Figure 5.** Optimized geometries of products computed at the B3LYP/6-31G(d) level.

of 40.83 kcal/mol to form **INT5**. Then **INT5** can go through three different pathways to form allene, propyne and 1-butene. The H atom on the center C can migrate toward  $\text{CH}_3$  to form the allyl radical and methane via a three-member-ring transition state **TS11** with an energy barrier of 30.28 kcal/mol. The allyl radical is ready to form propyne via H-elimination with a dissociation energy of 35.68 kcal/mol. Allene can be formed from the direct dissociation of the allyl radical as well, whose dissociation energy is slightly higher than that of propyne formation. Thus propyne can be formed more easily compared to allene, which is accordance with experimental results shown in part 1.<sup>12</sup> **INT5** can form the 2-butyl radical via the migration of the  $\text{CH}_3$  group, and the activation energy is calculated to be 60.08 kcal/mol. Then 1-butene is formed by H-elimination from the 2-butyl radical. On the other hand, **INT5** can form **INT6** by H-elimination with a dissociation energy of 40.32 kcal/mol. Then 1-butene is formed via a transition state **TS13** from **INT6**, which is another formation pathway of 1-butene with an activation energy of 92.56 kcal/mol. Due to the high energy barrier, the second channel of 1-butene is unimportant.

**3.2.2. Decomposition of Isobutene.** Figure 7 displays six reaction pathways of isobutene, containing three direct dis-

sociation channels to form 2-methylallyl,  $(\text{CH}_3)_2\text{C}=\text{CH}$  and  $\text{CH}_2=\text{CCH}_3$  radicals, and three channels via transition states to yield 1-butene, propyne and allene, respectively. Moreover, the further reaction pathways of 1-butene and isomerization of propyne to allene are also shown in Figure 7. (1) Isobutene can form the 2-methylallyl radical via C–H bond fission in one  $\text{CH}_3$  group of isobutene with a dissociation energy of 88.38 kcal/mol. (2) Isobutene can also form the  $(\text{CH}_3)_2\text{C}=\text{CH}$  radical via the C–H bond fission of the  $\text{CH}_2$  group with a dissociation energy of 111.17 kcal/mol. Compared with channel 1, channel 2 is unfavorable kinetically. (3) C–C bond cleavage between central C and  $\text{CH}_3$  in isobutene is more difficult than C–H bond fission in channel 1. The C–C bond dissociation energy is 97.48 kcal/mol. (4) One H atom of  $\text{CH}_3$  in isobutene can migrate toward the C atom of the other  $\text{CH}_3$  to produce allene and methane via a four-center transition state **TS14** with a barrier of 111.14 kcal/mol. (5) Isobutene can undergo a transition state **TS15**, surmounting a barrier of 121.24 kcal/mol to dissociate to propyne and methane. The isomerization of propyne to allene need undergo **TS16** with a barrier of 82.43 kcal/mol. The formation of both allene and propyne from isobutene need higher energy than from the *tert*-butyl radical, as shown in Figure 6. Thus the dominant formation pathways of allene and propyne should be from dissociation of the *tert*-butyl radical. (6) The barrier of isomerization of isobutene to 1-butene is 88.89 kcal/mol (**TS17**). Compared with the 1-butene formation channel from the *tert*-butyl radical shown in Figure 6, the isomerization is not the main pathway for 1-butene formation. At high temperature, 1-butene can decompose to  $\text{C}_4\text{H}_7$  radical (1-buten-3-yl radical and but-3-en-1-yl radical). The dissociation energy of 1-butene to 1-buten-3-yl radical ( $\text{CH}_2=\text{CHCHCH}_3$ ) is 84.00 kcal/mol, 16.28 kcal/mol lower than that of 1-butene to the but-3-en-1-yl radical ( $\text{CH}_2=\text{CHCH}_2\text{CH}_2$ ). 1-Buten-3-yl radical forms 1,3-butadiene by further H-elimination. 1-Butene can also undergo a transition state **TS18**, surmounting an activation energy of 108.23 kcal/mol to form 1,3-butadiene and hydrogen at higher temperature.

**3.2.3. Decomposition of Methanol.** Three consumption channels of methanol are displayed in Figure 8. First, methanol can undergo a four-member-ring transition state **TS19** with an activation energy of 91.02 kcal/mol to produce formaldehyde and hydrogen. The initial formation of formaldehyde should come from H-elimination of the methoxy radical rather than from  $\text{H}_2$ -elimination of methanol, because the dissociation energy of the former pathway is 5.15 kcal/mol lower than that of the latter one. But both formation pathways of formaldehyde compete with each other at high temperature. CO can be formed from further H-elimination of formaldehyde. Second, hydroxymethyl radical can be formed by methanol homolysis with a dissociation energy of 95.67 kcal/mol. The hydroxymethyl radical is not detected in our experiment. The reason could be that the reaction of the hydroxymethyl radical with the methyl radical is very fast. Finally, methanol can form the methoxy radical via O–H homolysis with a higher dissociation energy (104.17 kcal/mol). Compared with dissociation of MTBE to the methoxy radical, the decomposition of methanol to the methoxy radical has less contribution. Furthermore, the methoxy radical is isomerized to the hydroxymethyl radical by undergoing a three-member-ring transition state **TS20** (29.96 kcal/mol). In comparison with the unimolecular decomposition of methanol reported by Lin and co-workers using the G2 M method,<sup>20</sup> the highest deviation of the G3B3 method is less than 0.73 kcal/mol in calculating above three decomposition channels of methanol. This also indicates that the G3B3 method is a more

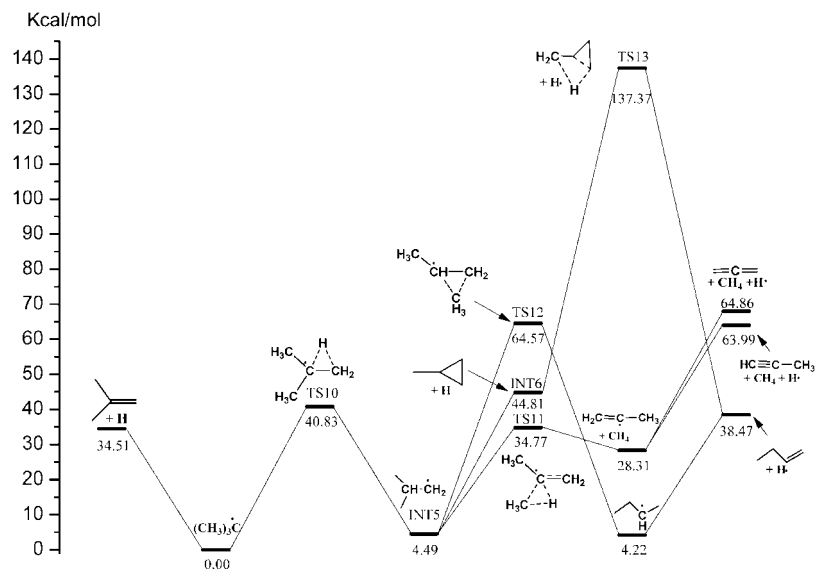


Figure 6. Relative energies of the species involved in the decomposition of the *tert*-butyl radical calculated at the G3B3 level of theory.

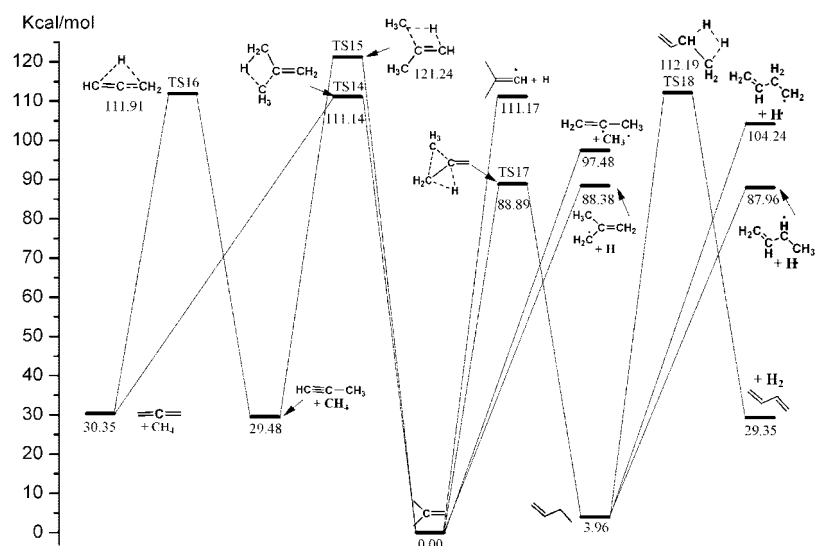


Figure 7. Relative energies of the species involved in the decomposition of isobutene calculated at the G3B3 level of theory.

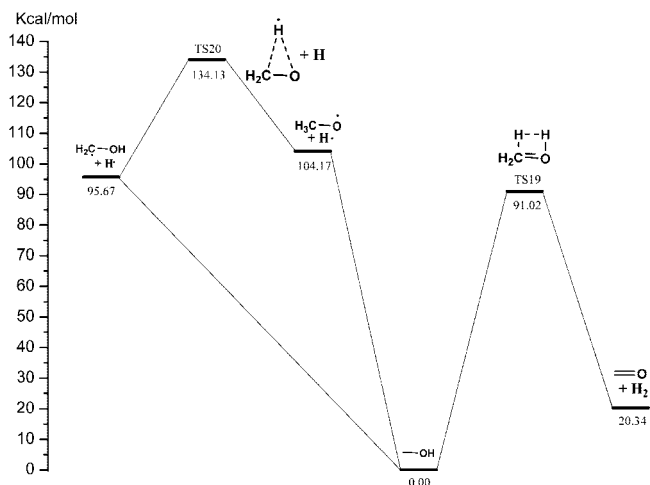
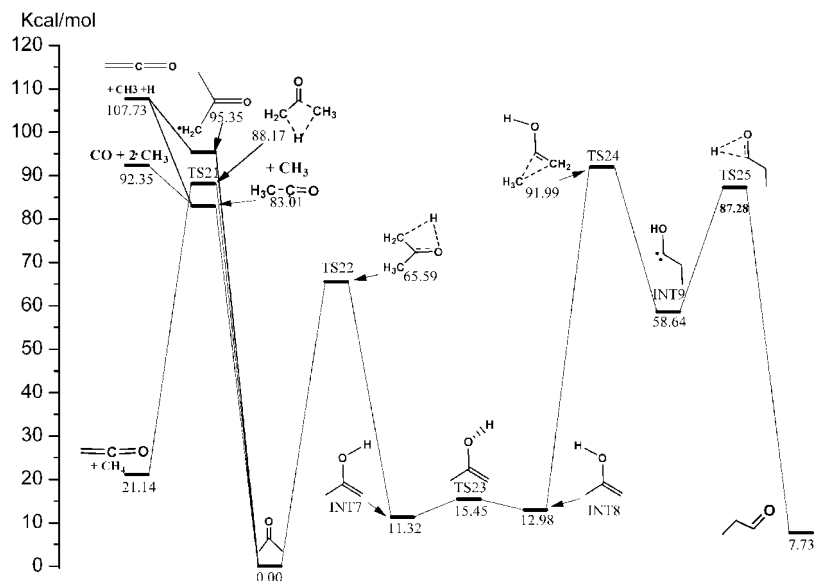


Figure 8. Relative energies of the species involved in the decomposition of methanol calculated at the G3B3 level of theory.

cost-effective method than G2M in such a case. The decomposition pathways of methanol proposed by Lin et al. contain some other pathways that were not calculated in this work in view of integrity of their work.

**3.2.4. Decomposition of Acetone.** Four consumption channels of acetone are displayed in Figure 9. (1) Acetone can undergo C–C bond homolysis to form the methyl and acetyl radicals with an energy of 83.01 kcal/mol, followed by dissociation of the acetyl radical yielding CO and another methyl. The dissociation of the acetyl radical to ketene and H can occur with an energy barrier of 24.72 kcal/mol. Our result is in good agreement with Sato et al.'s conclusion that C–C bond cleavage to form the methyl and acetyl radicals is the lowest energy pathway for decomposition of acetone.<sup>22</sup> (2) Direct C–H cleavage of acetone can occur to yield 2-oxopropyl radical and H. The dissociation energy of this reaction is 95.35 kcal/mol. With additional 12.38 kcal/mol, the 2-oxopropyl radical can dissociate to ketene and methyl radical. (3) The H atom of one CH<sub>3</sub> group in acetone can migrate toward the C atom in another CH<sub>3</sub> group to produce ketene and methane via a four-center transition state **TS21** with an energy barrier of 88.17 kcal/mol. (4) The H atom of CH<sub>3</sub> in acetone can migrate toward the O atom to produce **INT7** via a four-center transition state **TS22** with an energy barrier of 65.59 kcal/mol. The internal rotation barrier of H–O bond from **INT7** to **INT8** via **TS23** is predicted to be 4.13 kcal/mol. Subsequently, **INT8** can undergo a three-



**Figure 9.** Relative energies of the species involved in the decomposition of acetone calculated at the G3B3 level of theory.

center-ring transition state **TS24** surmounting an activation energy of 79.01 kcal/mol to produce singlet **INT9**. The H atom of hydroxy in **INT9** can rapidly migrate toward the closest C atom to produce propanal via a three-center-ring transition state **TS25** with an activation energy of 28.64 kcal/mol. Propanal can further eliminate  $H_2$  to form 2-propenal. As far as we know, the relative energies of formation of ketene from acetone and isomerization of acetone to propanal have not been reported.

Pyrolysis pathways can be elucidated more clearly with theoretical calculations discussed above than by simplex deduction from experimental results. As mentioned above, isobutane is mainly formed by recombination of the *tert*-butyl radical and H. Moreover, the calculation is also helpful to decide some species that are not identified in the experimental work. For example, the  $C_4H_7$  radical contains two isomers, 2-methylallyl radical and 1-buten-3-yl radical, that are not distinguished in the experimental work because of weak signals. In view of  $C_5H_{10}$  formation from recombination of  $C_4H_7$  with  $CH_3$ , the  $C_5H_{10}$  should comprise 2-methyl-1-butene and 3-methyl-1-butene at least.

#### 4. Conclusion

Theoretical study of MTBE pyrolysis has been performed with the G3B3 method. On the basis of the experimental results in part 1 and theoretical calculations in this work, the detailed pyrolysis channels are supplied, especially the primary and secondary pyrolysis reactions. The primary decomposition pathways include direct bond-cleavages and reactions via transition states: (1) Methanol and isobutene can be formed via a four-member-ring transition state with the lowest energy barrier, which is in good agreement with the experimental measurement. (2)  $CH_4$  elimination reaction can produce an intermediate **INT3** and 2-butanone. (3) The lowest energy pathway of  $H_2$ -elimination is dissociation of MTBE to isobutene, formaldehyde and  $H_2$  via a six-member-ring **TS4**. (4) C–O bond-cleavage reactions in different positions form the *tert*-butyl + methoxy radicals and the *tert*-butoxyl (**INT1**) +  $CH_3$  radicals, respectively. (5)  $(CH_3)_2COCH_3$  (**INT2**) and  $CH_3$  radicals can be formed from C–C bond-cleavage reaction. (6) Three C–H bond cleavages in different  $CH_3$  groups have relatively high dissociation energies as compared to the C–O and C–C bond cleavages. The primary pyrolysis products can undergo thermal

decompositions to form other species. Among the secondary reactions, propyne and allene are readily formed from decomposition of the *tert*-butyl radical via an intermediate allyl radical. The isomerization of isobutene to 1-butene is a secondary pathway for 1-butene formation, relative to the decomposition of the *tert*-butyl radical. The study of pyrolysis channels of MTBE enriches the high temperature chemistry of MTBE and related intermediates.

**Acknowledgment.** F.Q. is grateful for the funding supports from Chinese Academy of Sciences, the Specialized Research Fund for the Doctoral Program of Higher Education, Natural Science Foundation of China under Grant no. 20533040, National Basic Research Program of China (973) under Grant no. 2007CB815204 and Ministry of Science and Technology of China under Grant no. 2007DFA61310.

#### References and Notes

- (1) Choo, K. Y.; Golden, D. M.; Benson, S. W. *Int. J. Chem. Kinet.* **1974**, *6*, 631.
- (2) Chambreau, S. D.; Zhang, J. S.; Traeger, J. C.; Morton, T. H. *Int. J. Mass Spectrom.* **2000**, *199*, 17.
- (3) Brocard, J. C.; Baronnet, F.; O'Neal, H. E. *Combust. Flame* **1983**, *52*, 25.
- (4) Ciajolo, A.; Danna, A.; Kurz, M. *Combust. Sci. Technol.* **1997**, *123*, 49.
- (5) Norton, T. S.; Dryer, F. L. *Proc. Combust. Inst.* **1991**, *23*, 179.
- (6) Dunphy, M. P.; Simmie, J. M. *Combust. Sci. Technol.* **1989**, *66*, 157.
- (7) Curran, H. J.; Dunphy, M. P.; Simmie, J. M.; Westbrook, C. K.; Pitz, W. J. *Proc. Combust. Inst.* **1992**, *24*, 769.
- (8) Bohm, H.; Baronnet, F.; El Kadi, B. *Phys. Chem. Chem. Phys.* **2000**, *2*, 1929.
- (9) Yao, C. D.; Li, J.; Li, Q.; Huang, C. Q.; Wei, L. X.; Wang, J.; Tian, Z. Y.; Li, Y. Y.; Qi, F. *Chemosphere* **2007**, *67*, 2065.
- (10) Franklin, P. M.; Koshland, C. P.; Lucas, D.; Sawyer, R. F. *Chemosphere* **2001**, *42*, 861.
- (11) Atadinc, F.; Selcuki, C.; Sari, L.; Aviyente, V. *Phys. Chem. Chem. Phys.* **2002**, *4*, 1797.
- (12) Zhang, T. C.; Wang, J.; Yuan, T.; Hong, X.; Zhang, L. D.; Qi, F. *J. Phys. Chem. A* **2008**, *112*, 10487.
- (13) Baboul, A. G.; Curtiss, L. A.; Redfern, P. C.; Raghavachari, K. *J. Chem. Phys.* **1999**, *110*, 7650.
- (14) Curtiss, L. A.; Raghavachari, K.; Redfern, P. C.; Rassolov, V.; Pople, J. A. *J. Chem. Phys.* **1998**, *109*, 7764.
- (15) Frisch, M. J.; Trucks, G. W.; Schlegel, H. B.; Scuseria, G. E.; Robb, M. A.; Cheeseman, J. R.; Zakrzewski, V. G.; Montgomery, J. A., Jr.; Stratmann, R. E.; Burant, J. C.; Dapprich, S.; Millam, J. M.; Daniels, A. D.; Kudin, K. N.; Strain, M. C.; Farkas, O.; Tomasi, J.; Barone, V.;

Cossi, M.; Cammi, R.; Munnucci, B.; Pomelli, C.; Adamo, C.; Cliford, S.; Ochterski, J.; Petersson, G. A.; Ayala, P. Y.; Cui, Q.; Morokuma, K.; Rega, N.; Salvador, P.; Dannenberg, J. J.; Malick, D. K.; Rabuck, A. D.; Raghavachari, K.; Foresman, J. B.; Cioslowski, J.; Ortiz, J. V.; Baboul, A. G.; Stefanov, B. B.; Liu, G.; Liashenko, A.; Piskorz, P.; Komaromi, I.; Gomperts, R.; Martin, R. L.; Fox, D. J.; Keith, T.; Al-Laham, M. A.; Peng, C. Y.; Nakayakkara, A.; Challacombe, M.; Gill, P. M. W.; Johnson, B.; Chen, W.; Wong, M. W.; Andres, J. L.; Gonzalez, C.; Challacombe, M.; Gill, P. M. W.; Johnson, B.; Chen, W.; Wong, M. W.; Andres, J. L.; Gonzales, C.; Head-Gordon, M.; Replogle, E. S.; Pople, J. A. *Gaussian 03*, Revision C. 02 ed.; Gaussian, Inc.: Pittsburgh, PA, 2004.

(16) Knyazev, V. D.; Dubinsky, I. A.; Slagle, I. R.; Gutman, D. *J. Phys. Chem.* **1994**, *98*, 5279.

- (17) Zheng, X. B.; Blowers, P. *AIChE J.* **2006**, *52*, 3216.
- (18) Linstrom, P. J.; Mallard, W. G. NIST Chemistry WebBook; NIST Standard Reference Database Number 69; National Institute of Standards and Technology: Gaithersburg, MD, 2003.
- (19) Santhanam, S.; Kiefer, J. H.; Tranter, R. S.; Srinivasan, N. K. *Int. J. Chem. Kinet* **2003**, *35*, 381.
- (20) Xia, W. S.; Zhu, R. S.; Lin, M. C.; Mebel, A. M. *Faraday Discuss.* **2001**, *119*, 191.
- (21) Aronowitz, D.; Naegeli, D. W.; Glassman, I. *J. Phys. Chem.* **1977**, *81*, 2555.
- (22) Sato, K.; Hidaka, Y. *Combust. Flame* **2000**, *122*, 291.

JP8036268